

See discussions, stats, and author profiles for this publication at: <https://www.researchgate.net/publication/8329282>

Crystal structures of collagen model peptides with Pro-Hyp-Gly repeating sequence at 1.26 Å resolution: Implications for proline ring puckering

ARTICLE *in* BIOPOLYMERS · JANUARY 2004

Impact Factor: 2.39 · DOI: 10.1002/bip.20107 · Source: PubMed

CITATIONS

75

READS

43

8 AUTHORS, INCLUDING:



Kenji Okuyama

Osaka University

192 PUBLICATIONS 3,274 CITATIONS

SEE PROFILE

Kenji Okuyama¹

Chizuru Hongo¹

Rie Fukushima¹

Guanghan Wu¹

Hiroataka Narita¹

Keiichi Noguchi¹

Yuji Tanaka²

Norikazu Nishino²

¹ Faculty of Technology,
Tokyo University of Agriculture
and Technology,
Koganei, Tokyo 184-8588,
Japan

² Faculty of Engineering,
Kyushu Institute of
Technology,
Kitakyushu 804-8550, Japan

Received 19 December 2003;

accepted 27 April 2004

Published online 23 June 2004 in Wiley InterScience (www.interscience.wiley.com). DOI 10.1002/bip.20107

Crystal Structures of Collagen Model Peptides with Pro-Hyp-Gly Repeating Sequence at 1.26 Å Resolution: Implications for Proline Ring Puckering

Abstract: Triple-helical structures of (Pro-Hyp-Gly)*n* (*n* = 10, 11) at 100 K and room temperature (RT) were analyzed at 1.26 Å resolution by using synchrotron radiation data. Totals of 49 and 42 water molecules per seven triplets in an asymmetric unit were found for the structures at 100 K and RT, respectively. These water molecules were classified into two groups, those in the first and second hydration shells. Although there was no significant difference between water molecules in the first shell at 100 K and those at RT, a significant difference between those in the second shell was observed. That is, the number of water molecules at RT decreased to one half and the average distance from peptide chains at RT became longer by about 0.3 Å. On the other hand, of seven triplets in an asymmetric unit, three proline residues at the X position at 100 K clearly showed an up-puckering conformation, as opposed to the recent propensity-based hypothesis for the stabilization and destabilization of triple-helical structures by proline hydroxylation. This puckering was attributed to the interaction between proline rings and the surrounding water molecules at 100 K, which is much weaker at RT, as shown by longer average distance from peptide chains. © 2004 Wiley Periodicals, Inc. *Biopolymers* (Pept Sci) 76: 367–377, 2004

Keywords: collagen; crystal structure; hydroxyproline; triple helix

Correspondence to: Kenji Okuyama; e-mail: okuyamak@cc.tuat.ac.jp

Biopolymers (Peptide Science), Vol. 76, 367–377 (2004)

© 2004 Wiley Periodicals, Inc.

INTRODUCTION

Collagen is the most abundant protein in animals and is mainly responsible for structural integrity in their bodies. It has a very characteristic amino acid composition and sequence. That is, a glycyl residue (Gly) appears in every third position in its amino acid sequence, so that its sequence represents the repetition of a Gly-X-Y triplet. Furthermore, collagen has high imino acid contents (ca. 20%) compared with other proteins, especially proline (Pro) at X and 4(R)-hydroxyproline (Hyp, or 4(R)-Hyp where discrimination from its stereoisomer 4(S)-Hyp is needed) at the Y position. Because of these characteristic sequence constraints, collagen has a very unique triple-helical structure. After various proposals of different types of collagen model structures, the first triple-helical structure was proposed by Ramachandran and Kartha,¹ which was corrected slightly by Rich and Crick.^{2,3} This structure was known as the Rich and Crick model, or the 10/3-helical model, in which three peptide chains are assembled around the common axis and each of the three has 10 units of Gly-Pro-Hyp triplet and one helical turn in a fiber repeating period of 85.8 Å. On the other hand, we have proposed a 7/2-helical model based on the model peptide conformation found in the (Pro-Pro-Gly)₁₀ (hereafter, PPG10) single crystal.^{4,5} Since there was no convenient method of obtaining the initial model structure, this structure was analyzed by using the linked-atom least-squares method for fibrous polymers,⁶ even though three-dimensional reflection data were obtained. In this fiber diffraction analysis, the main refinement parameters were dihedral angles, ϕ , ψ , and ω , in a helical asymmetric unit of Pro-Pro-Gly.

In 1994, the structure of the collagen model peptide (Pro-Hyp-Gly)₄-(Pro-Hyp-Ala)-(Pro-Hyp-Gly)₅ (hereafter the Gly→Ala peptide) was analyzed by using protein crystallography.⁷ In this analysis, the refinement parameters were the positional and temperature parameters of peptide atoms and bound water oxygen atoms in a crystallographic asymmetric unit. Following this analysis, many structure analyses of collagen model peptides were reported from several groups, including (Pro-Hyp-Gly)₄-(Glu-Lys-Gly)-(Pro-Hyp-Gly)₅ (hereafter the EKG peptide),⁸ (Pro-Hyp-Gly)₃-(Ile-Thr-Gly-Ala-Arg-Gly-Leu-Ala-Gly-Pro-Hyp-Gly)-(Pro-Hyp-Gly)₃ (hereafter the T3-785 peptide),⁹ PPG10,^{10–13} and (Pro-Hyp-Gly)₁₀ (hereafter, POG10).^{14,15} The triple-helical structures of these model peptides at high resolution have provided much important structural information about collagen, such as the average helical symmetry of the peptide chain,

the location of bound water molecules around the triple helix, and proline ring puckering.

The 4(R)-Hyp residue appears preferentially at the Y position in the Gly-X-Y triplet, since prolyl-4-hydroxylase catalyses the posttranslational hydroxylation of proline residues at the Y position in the collagen sequence. This hydroxylation of proline residues is essential for the stabilization of the collagen triple helix. Ascorbic acid is required for full activity of prolyl hydroxylase and lack of this vitamin causes scurvy. The stabilization of the triple helix by Hyp is very clear from the difference in the helix-coil transition temperatures of PPG10 (25°C) and POG10 (58°C).¹⁶ This stabilization was once explained by the water-mediated hydrogen bond between the hydroxyl oxygen of Hyp and the carbonyl oxygen of Gly in the same chain,^{17,18} and later by the inductive effect hypothesis proposed by Raines.¹⁹ However, the former hypothesis could not explain the further stabilization by Flp, which has a fluorine atom at the C γ of Hyp instead of a hydroxyl group and the latter hypothesis could not clearly explain the destabilization of the triple helix by Hyp at the X position. In fact, (Hyp-Pro-Gly)₁₀ cannot make a triple helix at room temperature.²⁰ Based on the precise PPG10 structure together with data retrieved from the Cambridge Structural Database, the propensity-based hypothesis was proposed to explain collagen stabilization and destabilization by Hyp.¹² According to this hypothesis, proline rings in the X position take “down” puckering and those at the Y position take “up” puckering. Here, “up” and “down” puckering correspond to the negative and positive values of χ_1 dihedral angles, respectively. According to the analysis of the Cambridge Structural Database, Pro residues could take both up and down puckering, while Hyp residues could take only up puckering.¹² Therefore, stabilization by Hyp at the Y position and destabilization at the X position can be explained reasonably by the above hypothesis. In this context, it is important to examine proline ring puckering in the triple-helical structure at high resolution. In fact, some exceptions at the Y position of PPG10^{10,11} and (Pro-Pro-Gly)₉²¹ (hereafter, PPG9) have already been reported. Additionally, in the recently investigated high-resolution structure of POG10, the puckering of Pro at the X position was not reported since the electron density was less well defined for Pro residues and did not allow an unambiguous interpretation of their puckering.¹⁵ Furthermore, it was shown that the acetyl-(Gly-Hyp-Thr)₁₀-NH₂ peptide forms a triple-helical conformation in aqueous solution at room temperature, even though it has 4(R)-Hyp residues at every X position.^{22,23} In these circumstances, we examined the proline ring

puckering of (Pro-Hyp-Gly)_n ($n = 10, 11$) at high resolution to obtain reliable information about ring puckering, since our previous analysis was performed at rather low resolution.¹⁴

MATERIALS AND METHODS

Peptide Synthesis and Crystallization

The peptide (Pro-Hyp-Gly)₁₁ (hereafter, POG11) was synthesized by a solid-phase method on phenylacetamidomethyl resin²⁴ with *tert*-butoxycarbonyl (Boc) chemistry. Boc-Gly-OH was attached to the resin and chain elongation was performed by fragment condensation using Boc-Gly-Pro-Hyp(Bzl)-OH. At each segment condensation, 2.0 eq of building blocks was used with 2-(1-hydroxybenzotriazole-1-yl)-1,1,3,3-tetramethyluroniumhexafluorophosphate (HBTU)/1-hydroxybenzotriazole (HOBt) as a coupling reagent. Removal of the Boc group was performed by 25% trifluoroacetic acid in dichloromethane treatment after each coupling step. The Kaiser ninhydrin test was used to monitor the coupling reaction.²⁵ Finally, Boc-Pro-Hyp(Bzl)-OH was condensed to complete the objective peptide sequence. The peptide resin was treated with anhydrous HF to release the peptide from the resin. The crude product was purified by Sephadex G-50 (40% acetic acid) and corresponding fractions were collected, concentrated, and lyophilized. Fast atom bombardment mass (FAB-MS) spectra gave corresponding peaks. POG10 was purchased from Peptide Institute, Inc. (Japan) and was used for crystallization without further purification.

The peptide solution consisted of POG11 (POG10) at a concentration of 2.5 (4.5) mg/mL, 8(10)% (v/v) acetic acid, and 1(0)% (w/v) sodium azide. As a reservoir solute, 1 mL of 25(22)% (w/v) polyethylene glycol 200 (PEG200) was used. A mixture of 3 μ L of peptide and 3 μ L of reservoir solution was used as a crystallization drop. Crystals suitable for crystallographic analyses were grown by the hanging drop method at 10°C (POG10) and 4°C (POG11) within a week. In an earlier study,¹⁴ we observed two types of crystal morphologies, triangular and rod-like shapes. In this study, however, only triangular crystals were obtained in both cases.

X-Ray Data Collection

X-ray data collection was performed at BL44XU (POG10) and BL40B2 (POG11) of the SPring-8 synchrotron radiation source by using 0.9 (POG10) and 1.0 Å (POG11) wavelengths. Diffraction data were recorded on an Oxford PX210 CCD detector system (BL44XU) and an ADSC Quantum 4 CCD system (BL40B2), with a total oscillation range of 180° and an oscillation angle of 1.0°. In order to measure strong intensities in the low angle region, two data sets with different exposure times and camera lengths (5 s and 174 mm; 2.5 s and 294 mm) were collected for one crystal because of the strong incident beam of BL44XU, while in the case of BL40B2, the exposure time and camera

length were fixed to 10 s and 100 mm, respectively. As a cryoprotecting agent, 20% (w/v) 2-methyl-2,4-pentanediol was used for the data collection at 100 K. Data collection statistics are reported in Table I.

Structure Refinement

As in previous analyses of PPG10^{5,10–13} and POG10,^{14,15} diffraction patterns of POG10 and POG11 contained a small number of weak reflections at both sides of strong reflections on the layer lines, corresponding to the fiber repeating period of 20 Å. In neither case could we determine the unit cell dimensions that could explain these weak reflections. Therefore, the structures were refined as an infinite helix model, following the same strategy used in previous refinements of PPG10^{10–12} and POG10.^{14,15} That is, only the reflections corresponding to a subcell with the *c*-axis of about 20 Å were used in each analysis. The refinement was carried out by using SHELX-L,²⁶ with the previously determined POG10 structure at 1.9 Å resolution¹⁴ as a starting model. An anisotropic treatment of the atomic displacement parameters was used for nonhydrogen atoms in peptides, while an isotropic treatment was used for water oxygen atoms. Five percent of the reflections were used for the R_{free} monitoring. Peaks in the Fo-Fc maps were identified as potential water sites using distance cutoff criteria and hydrogen bonding geometry. Only water molecules lowering *R* and R_{free} were retained. Refinement statistics are reported in Table I. Atomic coordinates have been deposited in the PDB (entry codes 1V7H for POG10 at 100 K, 1V4F for POG11 at 100 K, and 1V6Q for POG11 at RT).

RESULTS AND DISCUSSION

Peptide Main Chain Conformation and Helical Parameters

Three peptide main chain conformations found in this study were essentially the same and took a triple-helical structure very close to the ideal 7/2-helical model for collagen.⁴ As an example, the triple-helical conformation of POG11 at 100 K (POG11L_O) is shown in Figure 1. Hereafter, the data collection temperature and the initial of the first author of the paper were included in the abbreviation. Temperature was represented by “R” for room temperature (RT) and “L” for 100 K. In the case of a temperature between these, the closer one was used with a dash, such as PPG10R'_K1, which was measured at 259 K. Average ϕ , ψ , and ω conformation angles in the asymmetric seven triplets are listed in Table II together with those of two previous analyses, POG10R_N¹⁴ and POG10L_B.¹⁵ Geometrical features of helical mol-

Table I Data Collection Parameters and Refinement Statistics

	POG10L_O		POG11L_O	POG11R_O
(A) Data collection				
Device	Oxford PX210 CCD		ADSC Quantum 4R CCD	
Temperature (K)	100		100	293
Resolution limit (Å)	1.24	1.93	1.26	1.25
(last shell)	1.28–1.24	2.0–1.93	1.32–1.26	1.30–1.25
Number of unique reflections	2883	590	3592	3768
<i>R</i> _{merge} (last shell)	0.04(.06)	0.04(.14)	0.06(.19)	0.06(.24)
Completeness (last shell)	0.73(.74)	0.55(.10)	0.95(.79)	0.95(.68)
Mosaicity (°)	0.83	1.00	1.86	0.81
Space group	<i>P</i> 2 ₁		<i>P</i> 2 ₁	<i>P</i> 2 ₁
Unit cell dimensions				
<i>a</i> (Å)	13.89		13.86	14.05
<i>b</i> (Å)	26.12		26.18	26.78
<i>c</i> (Å)	19.95		19.89	20.00
β (°)	105.95		105.75	106.76
(B) Refinement statistics				
Resolution (Å)	10.0–1.25		10.0–1.26	10.0–1.25
Number of reflections	3176		3520	3733
No. of reflections (<i>F</i> > 4σ <i>F</i>)	3173		3395	3142
<i>R</i> _w / <i>R</i> _{free} (%)	12.7/18.3		13.2/15.7	12.7/18.0
Peptide nonhydrogen atoms	133		133	133
Water sites	49		49	42
Root mean square deviation (Å)				
1–2 Distance	0.016		0.055	0.018
1–3 Distance	0.026		0.024	0.023
Flat planes	0.037		0.034	0.031

ecules are well defined by the helical parameters unit height (h) and unit twist (θ) derived from the bond lengths, bond angles, and torsion angles by the method of Sugeta and Miyazawa.²⁷ The average unit height and unit twist are also listed at the bottom of Table II. Compared with the previous values at 1.9 Å resolution (POG10R_N), those obtained in this study were closer to the ideal unit twist ($\theta = 51.4^\circ$) for the 7/2-helical model. Root mean square deviations (RMSD) (0.06 Å) between two structures obtained at 100 K (POG10L_O and POG11L_O) showed very close resemblance. On the other hand, RMSD between structures obtained at RT (POG11R_O) and 100 K (POG11L_O and POG10L_O) were 0.21 and 0.19 Å, respectively, which showed little difference compared with RMSD between structures at 100 K. The previous structure (POG10R_N) has the smallest RMSD (0.19 Å) with POG11R_O, while it has 0.27 and 0.28 Å RMSD with POG10L_O and POG11L_O, respectively. These facts show that although the triple-helical structures at RT and 100 K are very similar, there is a small but significant difference between them.

Hydration of Triple Helices

The water content of PPG10 was estimated to be 46% from its density and X-ray diffraction data.²⁸ Since the volumes of the triple helices of POG11 and POG10 calculated from the unit cell volume and number of triple helices in the unit cell are very similar to those of PPG10, more or less similar numbers of water molecules are expected in asymmetric units of these crystals. However, in a previous analysis,¹⁴ we located only 17 water molecules without having unreasonable R_{free} . This rather small number of water molecules may be attributed to the low resolution of diffraction data, the low quality of a single crystal, and the temperature at which intensity data were collected. In this study, a total of 49 sites of water molecules were found in the asymmetric units of both structures measured at 100 K, while a total of 42 sites were found in the structures at RT. Of 49 water molecules in the POG10L_O crystal, 47 have their sites very close to those of the corresponding water molecules in the POG11L_O crystal. The maximum distance between corresponding water oxygen atoms was 0.44 Å.

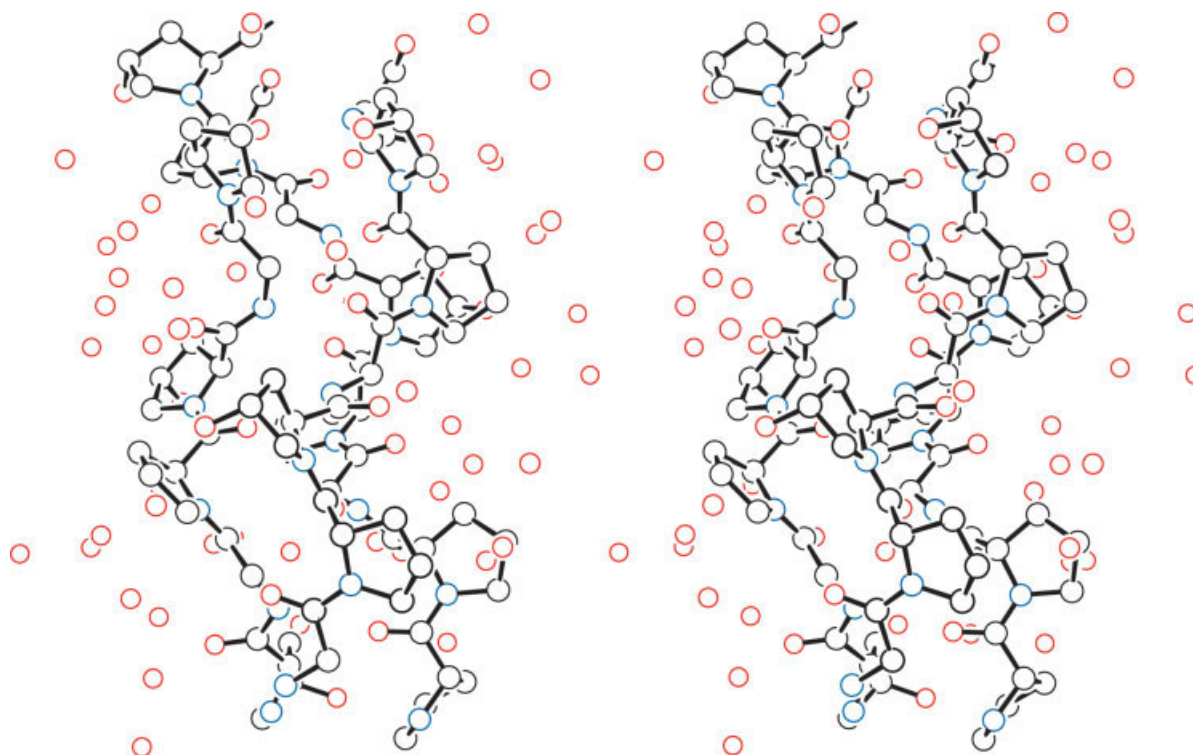


FIGURE 1 Molecular structure of POG11 at 100 K (POG11L_O) in an asymmetric unit together with 49 water molecules. The red, blue, and black open circles represent oxygen, nitrogen, and carbon atoms, respectively. For clarity, hydrogen atoms are not shown.

Table II Average Values of Main Chain Conformational Angles and Helical Parameters of Peptides with Pro-Hyp-Gly Repeating Sequences

Resolution (Å):	This study				
	POG11L_O 1.26	POG11R_O 1.25	POG10R_O 1.25	POG10R_N ¹⁴ 1.9	POG10L_B ¹⁵ 1.4
Conformational angles					
$\phi(\text{Pro})$	-70.0 (1.5)	-72.6 (1.6)	-71.3 (1.4)	-72.7 (3.5)	-69.8 (7.9)
$\psi(\text{Pro})$	162.3 (1.2)	163.7 (1.4)	161.5 (1.1)	161.6 (5.1)	162.0 (3.9)
$\omega(\text{Pro})$	172.3 (1.1)	174.5 (1.3)	172.3 (1.0)	179.6 (2.1)	— ^a
$\phi(\text{Hyp})$	-57.0 (1.4)	-57.4 (1.7)	-56.9 (1.3)	-58.4 (4.8)	-57.4 (2.0)
$\psi(\text{Hyp})$	149.6 (1.3)	151.8 (1.4)	150.0 (1.1)	152.0 (6.4)	149.8 (2.9)
$\omega(\text{Hyp})$	174.6 (1.3)	172.9 (1.4)	174.7 (1.1)	178.5 (2.1)	— ^a
$\phi(\text{Gly})$	-71.1 (1.8)	-72.5 (2.1)	-71.3 (1.6)	-74.8 (5.6)	-70.4 (3.8)
$\psi(\text{Gly})$	173.4 (1.3)	174.2 (1.5)	174.2 (1.2)	172.8 (3.0)	174.9 (3.4)
$\omega(\text{Gly})$	178.7 (1.2)	179.4 (1.4)	178.8 (1.1)	179.2 (1.7)	— ^a
Helical parameters					
$h/\text{Å}$	8.44	8.10	8.46	8.45	
$\theta/^\circ$	51.9	53.7	51.9	46.5	

^a Data not shown in Berisio et al.¹⁵

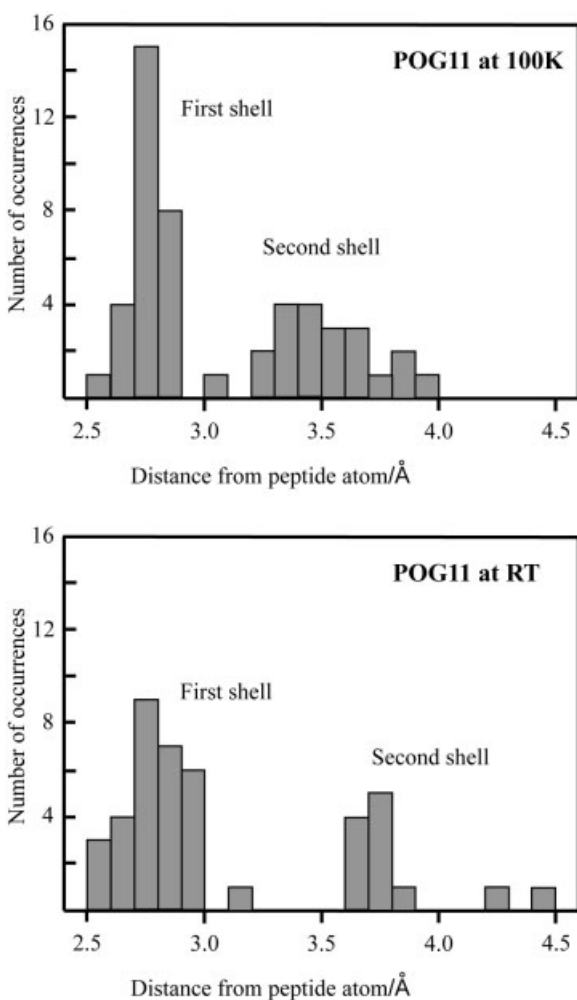


FIGURE 2 Distribution of water molecules in an asymmetric unit along the radial direction from the closest peptide atom found in the POG11 crystal at 100 K (above) and at RT (below).

The remaining 2 water molecules deviated by 1.1 and 1.3 Å from the corresponding ones in the other crystal.

The number of water molecules is plotted against the closest distance to a peptide atom in Figure 2. Since the result for POG10_O was very similar to that for POG11L_O, only the results of the latter and POG11R_O are shown. These water molecules were classified into two groups, those in the first and second hydration shells (Figure 2). The former water molecules link to the peptide oxygen atoms by direct hydrogen bonds. The numbers of water molecules in the first shell are 29 (POG10L_O and POG11L_O) and 30 (POG11R_O). The corresponding water molecules in these three crystals occupy essentially the same positions in their crystal structures. They participate in hydrogen bonds with peptide oxygen atoms as follows. The carbonyl oxygen of Hyp has two hydro-

gen bonds with water molecules and that of Gly has one, since the other site for a hydrogen bond is stereochemically hindered by the neighboring peptide chain. On the other hand, the carbonyl oxygen of Pro is directed to the center of the triple helix and participates in a direct hydrogen bond with the NH of Gly in the neighboring chain, which results in no space for water molecules. The hydroxyl oxygen of Hyp also has two hydrogen bonds. Of seven Hyp in the asymmetric unit, five hydroxyl oxygen atoms have hydrogen bonds only with water molecules. The remaining two have one hydrogen bond with a water molecule and the other with a hydroxyl oxygen of Hyp in the neighboring triple helix. The latter makes a direct hydrogen bond between adjacent triple helices in the *a*-direction, as shown later. Distribution of water molecules around the peptide oxygen atoms in an asymmetric unit can be seen in Figure 3, where seven Gly-Hyp peptides are superposed together with water molecules in the first hydration shell. Some of these characteristic hydrogen bonding patterns of water molecules have already been reported in the structures of collagen model peptides.^{8-12,14,18,21}

The number of water molecules in the second hydration shell is 20 (49 – 29) at 100 K, while it is 12 (42 – 30) at RT. These water molecules linked to those in the first shell. The average distance of these water molecules at RT (3.83 Å) is away from the peptide atoms by about 0.3 Å compared with that (3.54 Å) at 100 K (Figure 2). On the other hand, no significant difference between average distances at RT and 100 K was observed for those in the first hydration shell (2.77 Å at 100 K and 2.79 Å at RT). That is, at RT, water molecules in the second hydration shell loosen their hydrogen bonds with those in the first hydration shell, while those in the first shell are not affected. This suggested that comparing the structure at 100 K, the hydrated state in the triple-

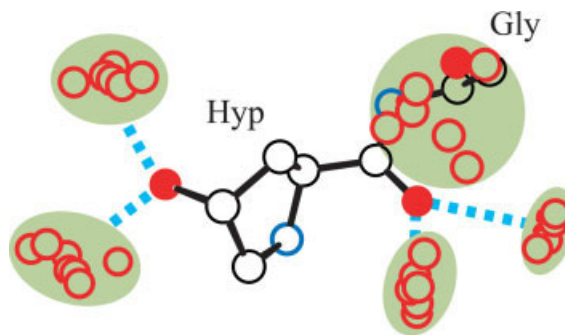


FIGURE 3 Distribution of water molecules in the first hydration shell. Water molecules (red open circles) in an asymmetric unit are superimposed on the Hyp-Gly dipeptide.

helical structure at RT becomes closer to that in an aqueous solution.

Most of the water oxygen atoms found in this study have tetrahedral coordination with other water oxygen atoms together with peptide oxygen atoms. For example, in structures at 100 K, 67% of water molecules (33 of 49) have four oxygen atoms and 31% (15 of 49) have three oxygen atoms within the hydrogen bonding distance. Since this statistic differs from that of a previous analysis, where 53% of water molecules had four neighbors and 39% had three,¹⁵ the precise atomic coordinates of water molecules of POG10L_O and POG11L_O found in this study seemed to be different from those of POG10L_B,¹⁵ even though the number of water molecules and the data collection temperature were the same. Different from the case of PPG10,¹³ no water molecule was found which belongs to the third hydration shell. From speculation about the water contents of PPG10,²⁸ the number of water molecules in an asymmetric unit was expected to be around 80 to 100. Therefore, one half of the sites for water molecules were defined and the other half did not show their specific sites.

Proline Ring Puckering

When precise triple-helical structures have been determined at high resolution, proline ring puckering is one of the most interesting structural findings, since it is directly related to the recent propensity-based hypothesis.¹² Proline ring puckering at the X and Y positions for (Pro-Hyp-Gly)_n and (Pro-Pro-Gly)_n peptides reported so far is summarized in Table III, where positive and negative values of χ_1 correspond to the down and up puckering of proline rings, respectively. The χ_1 values of the PPG10 crystal for the full cell structure with $c = 182 \text{ \AA}$ ¹³ are not listed here since the average values of the χ_1 angles at the corresponding residues in the full cell should be equal to those values in PPG10R_V.¹²

All the structures in Table III have seven triplets in an asymmetric unit. Therefore, there are seven independent positions for both X and Y. All the seven Hyp residues at the Y position showed up puckering, while proline rings at the X position in structures at 100 K take three up and four down puckering and that of POG11R_O has one up and six down puckering. In the high-resolution analysis of POG10L_B, the proline ring puckering at the X position was not cited because of the poor electron density around Pro residues.¹⁵ We also experienced low electron density of Pro residues in the POG10L_O structure. In the cases of POG11L_O and POG11R_O, however, electron densities of Pro residues were clear enough to deter-

mine ring puckering, as shown in Figure 4. Considering the clear evidence observed on the electron density map, the above ring puckering at the X position, evidence in opposition to the recent propensity-based hypothesis, is highly reliable. This experimental evidence suggested that the puckering at the X position was affected by the temperature at which diffraction data were measured. According to the NMR study of POG10 in an aqueous solution, proline residues at the X position had a down puckering conformation.²⁹ As cited in a previous section, the hydration state of the triple-helical structure in a single crystal at RT becomes closer to that of an isolated triple-helical structure in an aqueous solution. Therefore, change in the hydration state seems to be the main reason for the difference in puckering between 100 K and RT. That is, the opposing puckering at 100 K seemed to be attributed to the interaction between the proline ring and surrounding water molecules in the second hydration shell.

In the case of the Pro-Pro-Gly sequence, all the χ_1 values at the X position showed down puckering, which follows the hypothesis. However, of seven, one (PPG10R'_K1¹¹ and PPG9R_H²¹) or three (PPG10R_N¹⁰) Pro residues at the Y position take down puckering instead of up puckering. Since the resolutions of two analyses (PPG10R_N and PPG10R'_K1) are rather low compared with that of PPG10R_V,¹² and the results with PPG9R_H had not yet been published, the propensity-based hypothesis seems to be constructed without considering these findings. The Pro residues with marked χ_1 values at the Y position in the Pro-Pro-Gly sequence are located in identical positions in the lateral packing of triple helices. It is interesting to note that one down puckering residue in PPG10R'_K1 and PPG9R_H is located at the identical position in the lateral packing. Furthermore, the up puckering residues with rather small χ_1 values in the PPG10R_K2⁷ and PPG10R_V structures are also located at the identical position. This evidence seems to suggest that the interaction with neighboring triple helices via water molecules may affect proline ring puckering at the Y position in the Pro-Pro-Gly sequence. To understand these findings, we are now analyzing full cell structures of PPG9 at 100 K and RT at high resolution.

Packing Structure and Direct Hydrogen Bonds

Since three packing structures obtained in this study were very similar, only the structure of POG11L_O is shown in Figure 5, where triple helices are arranged laterally in a pseudo-hexagonal fashion. Plus marks in the region surrounded by the triple helices represent

Table III Conformational Angles of χ_1 of Proline Ring Puckering at the X and Y Positions in the X-Y-Gly Sequence

This study									
Temperature: Resolution (Å):	POG11L_O 100 K	POG11R_O RT	POG10L_O 100 K	PPG10R_N RT	PPG10R'_K1 259 K	PPG10R_K2 RT	PPG10R_V RT	PPG9R_H RT	POG10R_N RT
	1.26	1.25	1.25	1.9	1.97	1.60	1.30	1.0	1.9
χ ₁ at the X position									
X1	−20.0	16.0	−11.0	32.3	23.8	36.0	37.5	28.9	21.7
X2	−25.4	−6.5	−23.5	18.6	34.4	38.2	31.2	33.1	29.4
X3	13.5	15.0	16.4	26.8	0.9	31.4	29.3	24.5	20.6
X4	36.0	26.0	33.7	16.4	2.2	29.7	28.9	26.4	30.7
X5	34.5	11.4	25.2	37.0	27.6	35.5	29.2	26.5	25.7
X6	26.8	26.4	20.6	28.9	25.6	31.7	29.9	26.7	32.5
X7	−18.1	22.9	−16.3	29.2	23.6	35.8	30.0	28.9	31.0
χ ₁ at the Y position									
Y1	−25.6	−21.9	−27.9	−26.6	−10.1 ^a	−29.4	−22.5	−11.4	7.8 ^a
Y2	−24.6	−24.8	−24.2	−19.5	15.1	−34.9	−10.4	−19.4	−25.9
Y3	−24.9	−26.5	−24.8	−16.0	−14.2	−19.7	−14.9	−26.5	−24.5
Y4	−19.6	−20.7	−20.6	−20.5	22.0	−33.7	−26.1	−22.0	−18.7
Y5	−23.4	−24.3	−29.0	−24.5	−24.0	−26.6	−18.2	−21.6	−25.2
Y6	−24.4	−23.3	−25.4	−25.2	15.1	−30.3	−15.3	−13.2	−21.2
Y7	−25.2	−24.2	−26.2	−15.7	−12.2	25.5 ^a	−13.0 ^a	−9.0 ^a	−13.5

^a Y positions having marked χ_1 values in the Gly-Pro-Pro sequence are located in similar positions in lateral packing. Therefore, these Pro residues have similar interaction with adjacent triple helices.

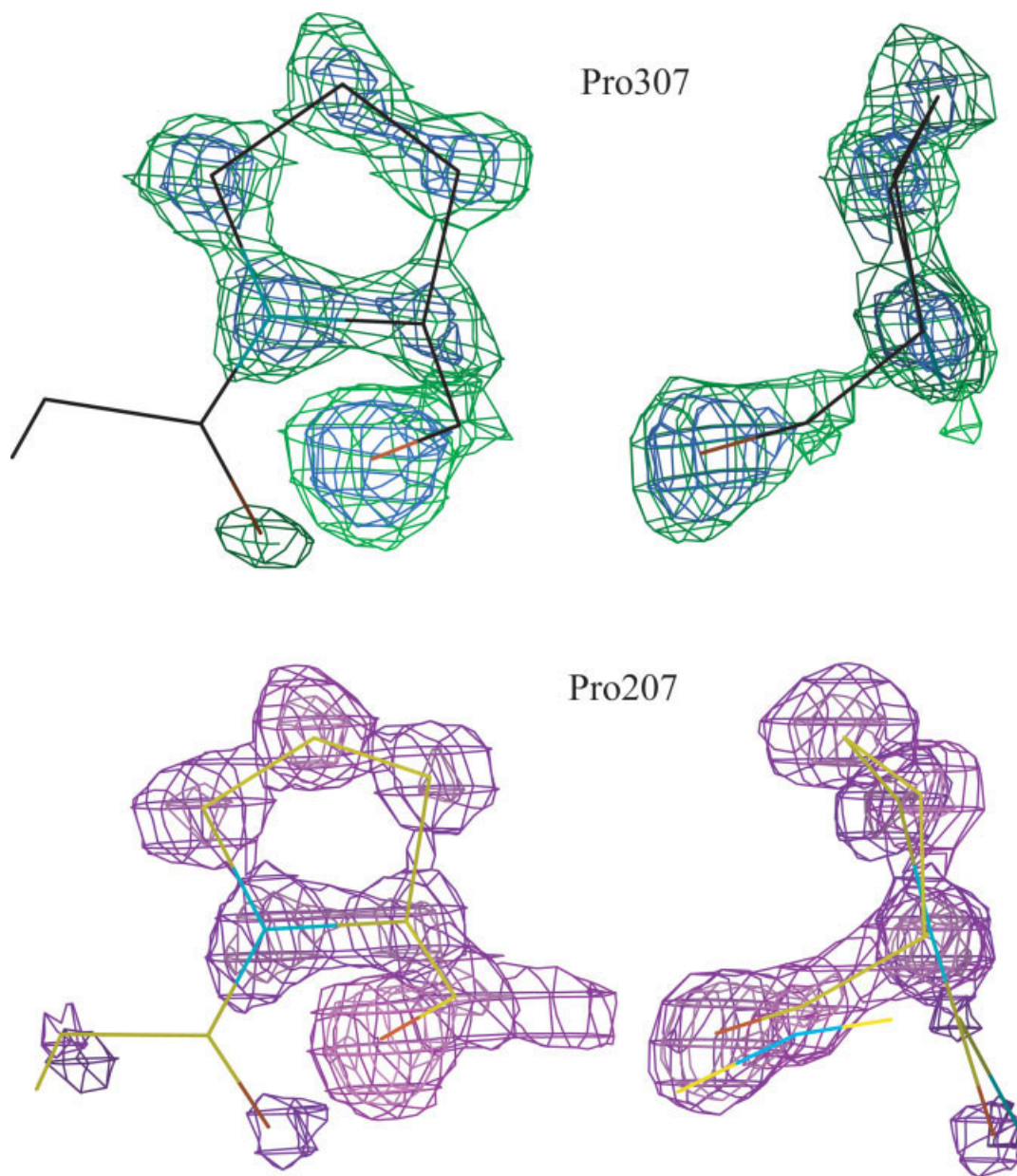


FIGURE 4 OMIT map of Pro307 (above) and Pro207 (below) of POG11 at 100 K clearly showing up and down puckering conformations, respectively.

water molecules found in this study. The triple helices along the *a*-axis are crystallographically identical and make a layer composed of molecules with the same direction. The adjacent layers are related to the first one by a crystallographic 2_1 -axis along the *b*-axis, which makes an alternate layer structure composed of the up and down triple helices. As shown by dotted lines, adjacent triple helices in one layer are directly linked by O-H...O hydrogen bonds between hydroxyl oxygen atoms of Hyp108 and Hyp202. The hydrogen bond lengths are 2.93 (POG11L_O), 2.71

(POG11R_O), and 2.88 Å (POG10L_O). This direct interaction between triple helices was first found in the crystal structure of the EKG peptide⁸ and later it was reported for the POG10L_B structure.¹⁵ We also recognized the short atomic distance between hydroxyl oxygen atoms of Hyp in adjacent triple helices of POG10R_N.¹⁴ However, since the resolution of this analysis was not high enough, we did not mention this interaction at that time. This hydrogen bond is only one direct interaction between adjacent triple helices and it occurs every 20 Å along the *c*-direction.

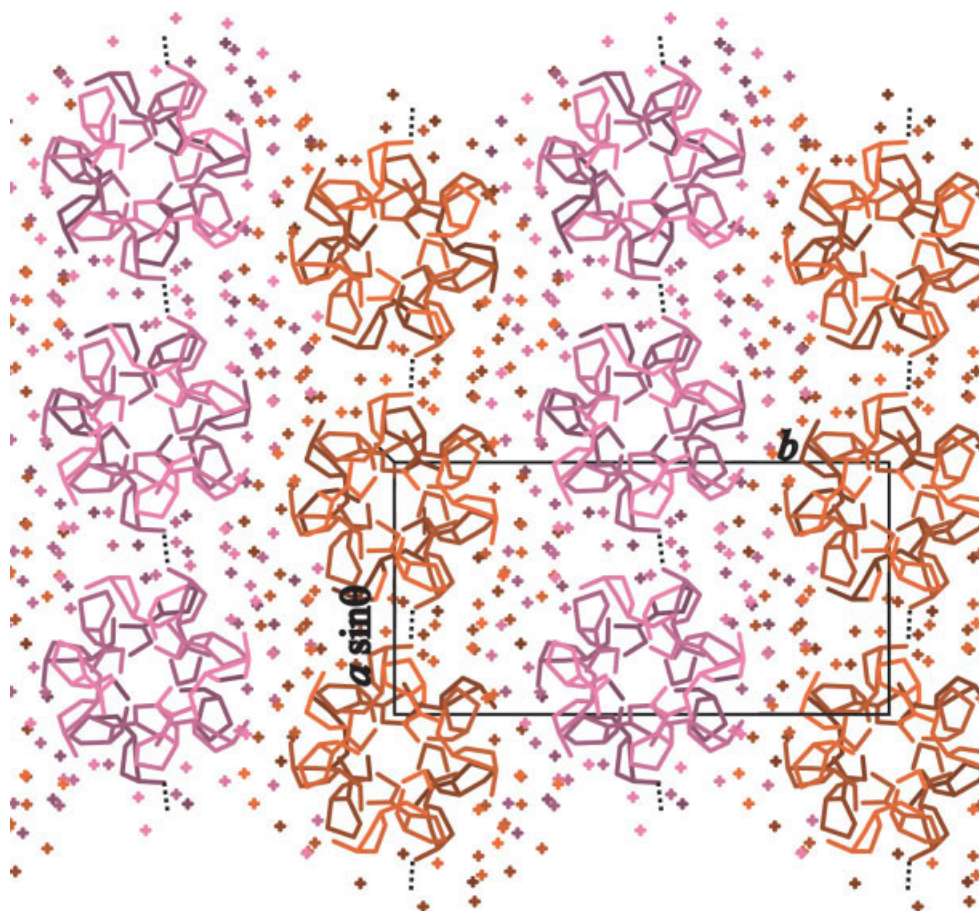


FIGURE 5 Lateral arrangement of POG11 at 100 K showing a pseudo-hexagonal packing. Adjacent triple helices along the b -axis are related by the crystallographic 2_1 symmetry in this direction. Plus marks represent water oxygen atoms. Dotted lines designate direct hydrogen bonds between hydroxyl oxygen atoms of Hyp in the adjacent triple helices along the a -axis.

The synchrotron radiation experiments were performed at the BL40B2 and BL44XU of the SPring-8 with the approval of the Japan Synchrotron Radiation Research Institute (JASRI).

REFERENCES

1. Ramachandran, G. N.; Kartha, G. *Nature (London)* 1955, 176, 593–595.
2. Rich, A.; Crick, F. H. C. *Nature (London)* 1955, 176, 915–916.
3. Rich, A.; Crick, F. H. C. *J Mol Biol* 1961, 3, 483–506.
4. Okuyama, K.; Takayanagi, M.; Ashida, T.; Kakudo, M. *Polym J* 1977, 9, 341–343.
5. Okuyama, K.; Okuyama, K.; Arnott, S.; Takayanagi, M.; Kakudo, M. *J Mol Biol* 1981, 152, 427–443.
6. Smith, P. J. C.; Arnott, S. *Acta Crystallogr* 1978, A34, 3–11.
7. Bella, J.; Eaton, M.; Brodsky, B.; Berman, H. M. *Science* 1994, 266, 75–81.
8. Kramer, R. Z.; Venugopal, M. G.; Bella, J.; Mayville, P.; Brodsky, B.; Berman, H. M. *J Mol Biol* 2000, 301, 1191–1205.
9. Kramer, R. Z.; Bella, J.; Brodsky, B.; Berman, H. M. *J Mol Biol* 2001, 311, 131–147.
10. Nagarajan, V.; Kamitori, S.; Okuyama, K. *J Biochem* 1998, 124, 1117–1123.
11. Kramer, R. Z.; Vitagliano, L.; Bella, J.; Berisio, R.; Mazzarella, L.; Brodsky, B.; Zagari, A.; Berman, H. M. *J Mol Biol* 1998, 280, 623–638.
12. Vitagliano, L.; Berisio, R.; Mazzarella, L.; Zagari, A. *Biopolymers* 2001, 58, 459–464.
13. Berisio, R.; Vitagliano, L.; Mazzarella, L.; Zagari, A. *Protein Sci* 2002, 11, 262–270.
14. Nagarajan, V.; Kamitori, S.; Okuyama, K. *J Biochem* 1999, 125, 310–318.
15. Berisio, R.; Vitagliano, L.; Mazzarella, L.; Zagari, A. *Biopolymers* 2001, 56, 8–13.

16. Berg, R. A.; Kishida, Y.; Kobayashi, Y.; Inoue, K.; Tonelli, A.; Sakakibara, S.; Prockop, D. J. *Biochim Biophys Acta* 1973, 328, 553–559.
17. Suzuki, E.; Fraser, R. D. B.; MacRae, T. P. *Int J Biol Macromol* 1980, 2, 54–56.
18. Bella, J.; Broadsky, B.; Berman, H. M. *Structure* 1995, 3, 893–906.
19. Holmgren, S. K.; Taylor, K. M.; Bretscher, L. E.; Raines, R. T. *Nature (London)* 1998, 392, 666–667.
20. Inouye, K.; Sakakibara, S.; Prockop, D. J. *Biochim Biophys Acta* 1976, 420, 133–141.
21. Hongo, C.; Nagarajan, V.; Noguchi, K.; Kamitori, S.; Okuyama, K.; Tanaka, Y.; Nishino, N. *Polym J* 2001, 33, 812–818.
22. Bann, J. G.; Bachinger, H. P. *J Biol Chem* 2000, 275, 24466–24469.
23. Mizuno, K.; Hayashi, T.; Bachinger, H. P. *J Biol Chem* 2003, 278, 32373–32379.
24. Mitchel, A. R.; Erickson, B. W.; Ryabtsev, M. N.; Hodges, R. S.; Merrifield, R. B. *J Am Chem Soc* 1976, 98, 7357–7362.
25. Kaiser, E.; Colescott, R. L.; Rossingor, C. D.; Cook, P. I. *Anal Biochem* 1970, 34, 595–598.
26. Sheldric, G. M.; Schneidern, T. R. *Methods Enzymol* 1997, 277, 319–343.
27. Sugeta, H.; Miyazawa, T. *Biopolymers* 1967, 5, 673–679.
28. Sakakibara, S.; Kishida, Y.; Okuyama, K.; Tanaka, N.; Ashida, T.; Kakudo, M. *J Mol Biol* 1972, 65, 371–373.
29. Li, M. H.; Fan, P.; Brodsky, B.; Baum, J.; Biochemistry 1993, 32, 7377–7387.